Bioorganic & Medicinal Chemistry 22 (2014) 1634–1641

Contents lists available at ScienceDirect

Bioorganic & Medicinal Chemistry

journal homepage: www.elsevier.com/locate/bmc

2,6-Diaminopurine nucleoside derivative of 9-ethyloxy-2-oxo-1,3-diazaphenoxazine (2-amino-Adap) for recognition of 8-oxo-dG in DNA

Yosuke Taniguchi *, Keitaro Fukabori, Yoshiya Kikukawa, Yohei Koga, Shigeki Sasaki *

Graduate School of Pharmaceutical Sciences, Kyushu University, 3-1-1 Maidashi, Higashi-ku, Fukuoka 812-8582, Japan

ARTICLE INFO

Article history:
Received 24 December 2013
Revised 14 January 2014
Accepted 18 January 2014
Available online 29 January 2014

Keywords:
Oxidative damage
8-Oxo-2′-deoxyguanosine
2-Oxo-1,3-diazaphenoxazine
Telomere
Fluorescent nucleoside
Light-up detection

ABSTRACT

8-Oxo-2′-deoxyguanosine (8-oxo-dG) is a nucleoside resulting from oxidative damage and is known to be mutagenic. 8-Oxo-dG has been related to aging and diseases, including neurological disorders and cancer. Recently, we reported that a fluorescent nucleoside derivative, adenosine-1,3-diazaphenoxazine (Adap), forms a stable base pair with 8-oxo-dG in DNA with accompanying efficient quenching. In this study, a new Adap derivative having an additional 2-amino group on the adenosine moiety (2-amino-Adap) was designed with the anticipation of additional hydrogen bonding with the 8-oxo group of 8-oxo-dG. The properties of the ODN containing 2-amino-Adap were evaluated by measuring thermal stability and fluorescence quenching. In contrast to the previously designed Adap, the base-pairing and fluorescence quenching properties of 2-amino-Adap varied depending on the ODN sequence, and there was no clear indication of an additional hydrogen bond with 8-oxo-dG. Instead, the base pairing of 2-amino-Adap with dG was significantly destabilized compared with that of Adap with dG, resulting in improved selectivity for 8-oxo-dG in the human telomere DNA sequence. Thus, the telomere-targeting ODN probe containing 2-amino-Adap displayed selective, sensitive and quantitative detection of 8-oxo-dG in the human telomere DNA sequence in a light-up detection system using SYBR Green.

1. Introduction

8-Oxo-2′-deoxyguanosine (8-oxo-dG) is ubiquitous in the nucleotide triphosphate pool and in DNA after exposure to ultraviolet radiation and oxidative stress.[1,2] 8-Oxo-dG is an inducer of genotoxicity during gene replication steps, which is in turn prevented by repair enzymes targeting 8-oxo-dGTP and 8-oxo-dG.[3] 8-oxo-dG is yet unaffected by the repair system to some extent, and it has been related to aging and diseases, such as neurological disorders and cancers. Several methods have been developed to measure 8-oxo-dG levels in biological samples, including HPLC–EDC,[4] HPLC–MS/MS,[5] GC–MS,[6] and immunoassays,[7] among others.[8] Fluorescent derivatives of 2-oxo-1,3-diazaphenoxazine (8-oxoG clamp) were developed by our group as the first recognition molecules for 8-oxo-dG in solution.[9] Recently, we reported that the adenosine derivative of 2-oxo-1,3-diazaphenoxazine (Adap) forms a selective base pair with 8-oxo-dG in DNA with accompanying effective fluorescence quenching.[10] Subsequently, Adap was applied to the light-emitting fluorescence detection of 8-oxo-dG by using a FRET-based Adap-masked probe.[11] Based on a plausible complex structure, shown in Figure 1A, in which Adap forms multiple hydrogen bonds on both the Hoogsteen face and the Watson-Crick face of 8-oxo-dG, we became interested in investigating the manner in which an additional 2-amino group on the adenosine moiety (2-amino-Adap in Fig. 1B) affects the recognition of 8-oxo-dG. It was also expected that the 2-amino group of the adenosine moiety might induce steric repulsion between the 2-amino group of guanosine in the *anti*-conformation in the minor groove,[12] thus potentially improving selectivity for 8-oxo-dG. In this paper, we describe in detail the synthesis and evaluation of oligonucleotides containing 2-amino-Adap.

2. Results and discussion

2.1. Synthesis of 2-amino-Adap and its oligonucleotides

The synthesis of 2-amino-Adap and the oligodeoxynucleotides (ODNs) are shown in Scheme 1. 2′-Deoxyguanosine (**1**) was protected by the 3′-*O*- and 5′-*O*-TBDMS groups and converted to the 2,4,6-triisopropylbenzenesulfonyl derivative (**2**). A substitution reaction was performed with the phenoxazine unit **3** in the presence of diisopropylethylamine to give TBS protected 2-amino-Adap

* Corresponding authors. Tel./fax: +81 92 642 6615.
E-mail addresses: taniguch@phar.kyushu-u.ac.jp (Y. Taniguchi), sasaki@phar.kyushu-u.ac.jp (S. Sasaki).

http://dx.doi.org/10.1016/j.bmc.2014.01.024
0968-0896/

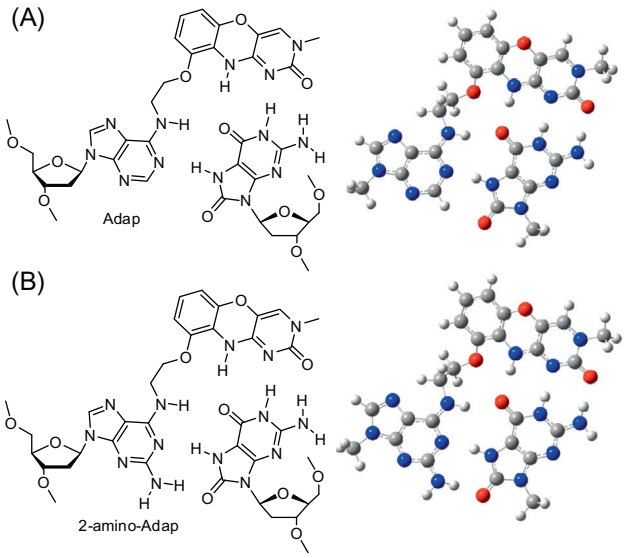

Figure 1. Expected recognition structure and model structure for base pair formation. (A) Adap:8-oxo-dG, (B) 2-amino-Adap:8-oxo-dG.

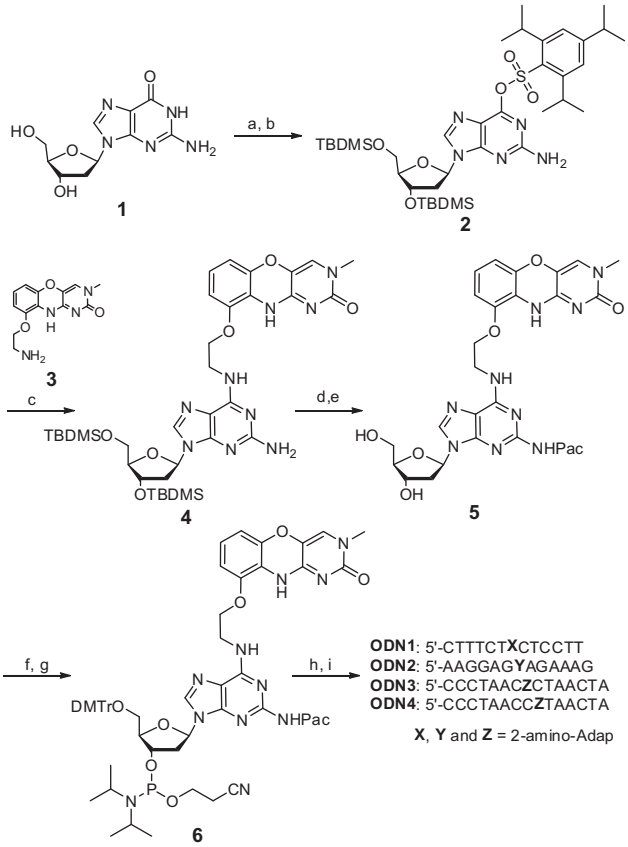

Scheme 1. Reagents and conditions: (a) TBDMSCl, imidazole, DMF, 73%; (b) TiPBSCl, Et_3N, DMAP, CH_2Cl_2, rt, 94%; (c) Phenoxazine unit 3, DIPEA, 1-propanol, reflux, 88%; (d) phenoxyacetylchloride, pyridine, 0 °C, 88%; (e) triethylamine–trihydrofluoride, THF, 90%; (f) DMTrCl, pyridine, rt, 64%; (g) 2-Cyanoethyl-*N*,*N*-diisopropylchlorophosphoramidite, DIPEA, CH_2Cl_2, 0 °C, 88%; (h) DNA synthesis; (i) HPLC purification, DMTr deprotection.

(**4**). The 2-amino group of **4** was protected with a phenoxyacetyl group, and the TBS groups were removed to produce compound **5**. Finally, **5** was converted to the corresponding phosphoramidite precursor (**6**) using the conventional method. The synthesized ODNs were cleaved from the CPG resin, and the Pac groups were deprotected in 28% aqueous ammonium solution at 55 °C for 6 h. The products were purified by HPLC and treated with 5% acetic acid to remove the DMTr-protecting group. The structure and purity of the synthesized ODNs were confirmed by MALDI-TOF analysis.

2.2. Thermal denaturing study of ODNs containing 2-amino-Adap

A thermal denaturing study was performed to determine T_m values using the 13 base pair duplex formed between ODN**1** and ODN**2** in a buffer containing 100 mM NaCl and 10 mM sodium phosphate buffer at pH 7.0. The T_m value at 2 μM of duplex DNA and thermodynamic parameters were obtained from van't Hoff plots with five data points and are summarized in Table 1.

The T_m value of the combination of X = 2-amino-Adap and Y = 8-oxo-dG was 47.6 °C, and the value for X = 8-oxo-dG and Y = 2-amino-Adap was 46.1 °C. These T_m values are equivalent to those for natural GC and AT base pairs. The T_m values for mismatched combinations were lower than those for the 2-amino-Adap and 8-oxo-dG pairs (X = 2-amino-Adap: T_m = 31.6, 35.6, 39.4 and 35.1 °C for dA, dC, T and dG, respectively. Y = 2-amino-Adap: T_m = 31.9, 33.0, 37.4 and 35.5 °C for dA, dC, T and dG, respectively.). To confirm a stabilizing effect of the diazaphenoxazine unit of 2-amino-Adap, the T_m values of ODN containing 2-amino-2′-deoxyadenosine (2-amino-dA) as a control base were measured. The combination of 2-amino-Adap and 8-oxo-dG gave higher T_m values than that of 2-amino-dA and 8-oxo-dG (40.2 °C vs 47.6 °C and 41.2 vs 46.1 °C), indicating that the diazaphenoxazine interacts with the Watson-Crick face of 8-oxo-dG in a *syn* conformation (Fig. 1B). These results show that 2-amino-Adap discriminates 8-oxo-dG from other nucleosides in a DNA duplex. However, it has not been clearly confirmed whether the 8-oxo-dG and 2-amino-Adap base pair is further stabilized by the additional 2-amino group in a duplex with homopyrimidine/homopurine context.

2.3. Fluorescence quenching property of 2-amino-Adap in ODNs

The fluorescence quenching property of 2-amino-Adap in ODNs was investigated by measuring the fluorescence spectra in the absence and presence of the complementary ODN using 50 nM of each ODN in a buffer containing 100 mM NaCl and 10 mM sodium phosphate at pH 7.0 and 30 °C. These spectra are illustrated in Figure 2. The fluorescence of 2-amino-Adap in ODN**1** was partly quenched by 8-oxo-dG in ODN**2** (Fig. 2A). Surprisingly, the fluorescence of 2-amino-Adap in ODN**1** was increased by the addition of dG-containing ODN**2** (Fig. 2B). In contrast, the fluorescence spectra of 2-amino-Adap in ODN**2** was effectively quenched by 8-oxo-dG in ODN**1** while retaining the same intensity when base-paired with dG in ODN**1** (Fig. 2C vs D). Based on the $\Delta G°$ values at 30 °C in Table 1, the duplex concentrations for each ODN combinations were calculated. In cases where the matched 2-amino-Adap and 8-oxo-dG combination was included (Fig. 2A and C), more than 95% of the fluorescent ODN**1** having 2-amino-Adap was estimated to be in the duplex form, which represented the fluorescence spectra shown in the red curve. In cases where the mismatched 2-amino-Adap and dG combination was included (Fig. 2B and D), 36–40% of the fluorescent ODN**2** having 2-amino-Adap was estimated to be in the duplex form. The red curves of these spectra contain contributions of these duplexes. In the previous study, the mismatched dG-Adap combination in the duplex DNA did not cause significant fluorescence quenching similarly with Figure 2D.[10] As the fluorescence intensity of 2-amino-Adap in ODN**1** is significantly weaker than in ODN**2** (Fig. 2A vs C), it is likely that 2-amino-Adap might be stacked within ODN**1** in a manner that causes fluorescence

Table 1
Thermodynamic parameters of 2-amino-Adap-containing ODNs complexed with complementary ODNs[a]

ODN**1** X	ODN**2** Y	T_m (°C)	$\Delta H°$ kcal/mol	$\Delta S°$cal/K mol	$\Delta G°_{30\ °C}$ kcal/mol
2-Amino-Adap	dA	31.6	−111 ± 14	−336 ± 46	−9.19 ± 0.3
2-Amino-Adap	dC	35.6	−94.9 ± 6	−278 ± 19	−10.7 ± 0.06
2-Amino-Adap	T	39.4	−80.6 ± 7	−228 ± 24	−11.5 ± 0.15
2-Amino-Adap	dG	35.1	−77.2 ± 3	−221 ± 8	−10.1 ± 0.02
2-Amino-Adap	8-Oxo-dG	47.6	−101 ± 6	−287 ± 17	−14.0 ± 0.2
dA	2-Amino-Adap	31.9	−132 ± 11	−405 ± 34	−9.29 ± 0.2
dC	2-Amino-Adap	33.0	−93.3 ± 6	−269 ± 18	−11.8 ± 0.1
T	2-Amino-Adap	37.4	−78.4 ± 5	−224 ± 17	−10.5 ± 0.08
dG	2-Amino-Adap	35.5	−82.9 ± 5	−240 ± 16	−10.2 ± 0.06
8-Oxo-dG	2-Amino-Adap	46.1	−107 ± 8	−306 ± 25	−14.3 ± 0.3
dC	dG	44.1	−101 ± 6	−288 ± 20	−13.4 ± 0.2
dG	dC	48.2	−115 ± 6	−328 ± 55	−15.3 ± 0.8
T	dA	40.9	−90.3 ± 7	−259 ± 22	−11.8 ± 0.2
dA	T	41.9	−92.9 ± 10	−266 ± 38	−12.3 ± 0.3
2-Amino-dA	dG	34.2	−75.0 ± 5	−215 ± 16	−9.86 ± 0.07
2-Amino-dA	8-Oxo-dG	40.2	−93.3 ± 6	−269 ± 18	−11.8 ± 0.09
dG	2-Amino-dA	33.5	−70.9 ± 3	−202 ± 10	−969 ± 0.03
8-Oxo-dG	2-Amino-dA	41.2	−95.7 ± 5	−276 ± 17	−12.1 ± 0.1

[a] UV melting profiles were measured using 2 μM of each ODN1 and ODN**2**. These values were determined by van't Hoff plots with five data points (1–8 μM) and the curve fitting method (Meltwin program). Thermodynamic data of natural base pairs are from Ref. 10b.

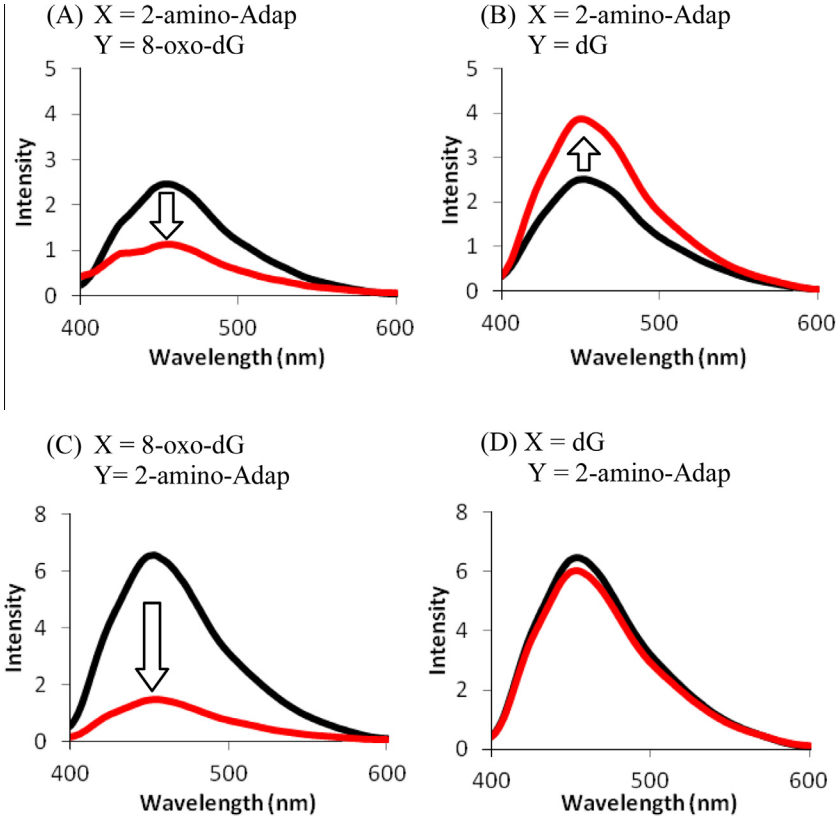

Figure 2. Fluorescence spectra of (A) 50 nM ODN**1**, 5′-CTTTCT**X**CTCCTT, and (B) 50 nM ODN**2**, 3′-GAAAGA**Y**GAGGAA, containing 2-amino-Adap with excitation at 365 nm in a buffer containing 100 mM NaCl and 10 mM sodium phosphate buffer at pH 7.0 and 30 °C. The black curves represent the spectra of single stranded ODN, and the red curves represent the results after the addition of complementary sequences.

quenching. Consequently, the increased fluorescence intensity shown in Figure 2B may be due to the relief of the intra-strand stacking by the formation of the duplex.

2.4. Recognition of 8-oxo-dG in telomere sequence

We next investigated recognition of 8-oxo-dG in the human telomere sequence using ODN**3** and ODN**4** with the complementary sequence. It has been reported that dG in the human telomere TAGTAG(TTAGGG)$_4$ repeat sequence is susceptible to oxidation to form 8-oxo-dG.[13] Examples of thermal melting curves are illustrated in Figure 3A. The duplex formed between telomere DNA**5** (X = dG, Y = 8-oxo-dG) and ODN**3** (Z = 2-amino-Adap) showed a higher T_m value than that with telomere DNA**6** (X = Y = dG) and ODN**3** (Z = 2-amino-Adap). The higher stability of the former duplex was also confirmed by a CD spectrum

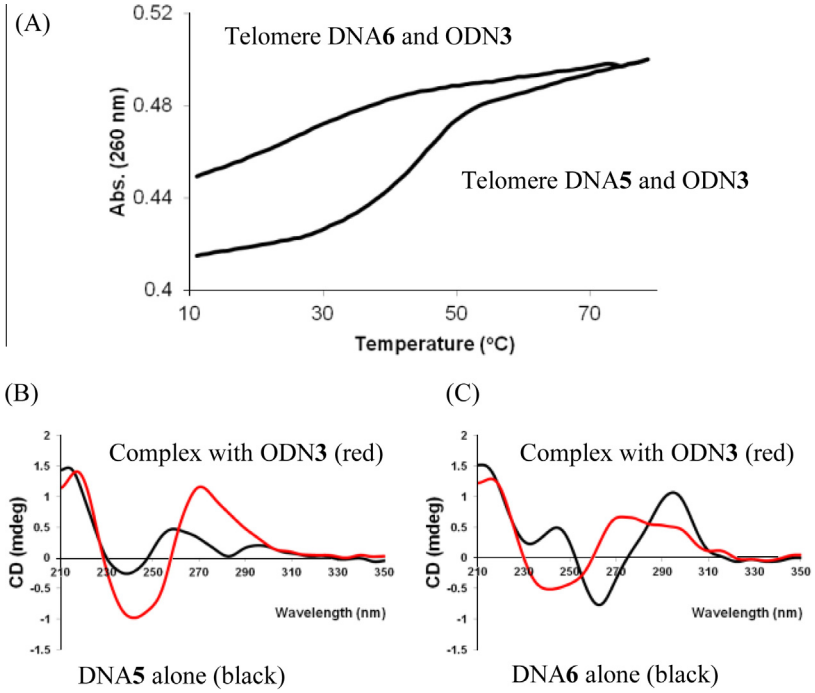

Figure 3. (A) Melting curves of the duplex formed between DNA**6** (dG) and ODN**3** ant that between DNA**5** (8-oxo-dG) and ODN**3** (2-amino-Adap). (B) CD spectra of DNA**5** (8-oxo-dG) alone (black curve) and the complex with ODN**3** (2-amino-Adap) (red curve). (C) CD spectra of DNA**6** (dG) alone (black curve) and complex with ODN**3** (2-amino-Adap) (red curve). Telomere DNA, 5′-TAGTAGTTA **X Y** GTTAGGG(TTAGGG)$_2$, in which DNA**5** contains X = dG and Y = 8-oxo-dG, DNA**6** contains X, Y = dG, and DNA**7** contains X = 8-oxo-dG, Y = dG.

(Fig. 3B, red curve), indicating a typical B-form conformation. The CD spectrum of telomere DNA**6** (X = Y = dG) alone resembled that of a G-quadruplex (Fig. 3C, black curve),[14] which was changed to a CD spectrum such that both B-type duplex and G-quadruplex are present (Fig. 3C, red curve).

The measured T_m values are summarized in Table 2. ODN**3** (2-amino-Adap) showed stable duplex formation with the telomere DNA**5** (X = dG, Y = 8-oxo-dG), as described previously (Table 2, Entry 1 and Fig. 3A). The duplex between ODN**3** (2-amino-Adap) and telomere DNA**6** (X = Y = dG) did not show a clear sigmoid curve (Table 2, Entry 2 and Fig. 3A). The T_m value for ODN**3** (2-amino-Adap) with telomere DNA**5** (X = dG, Y = 8-oxo-dG) was almost equal to that obtained with ODN**3** (Adap) (Table 2, Entries 1 and 5). The T_m value for the duplex formed between ODN**3** (2-amino-Adap) and telomere DNA**5** (X = dG, Y = 8-oxo-dG) was 19.2 °C higher than the value for the duplex formed with the telomere DNA**6** (X, Y = dG) when measured in a buffer containing 500 mM NaCl (Table 2, Entries 3 and 4). It was clear that 2-amino-Adap in ODN**3** formed a stable base pair with 8-oxo-dG in telomere DNA**5**, whereas the duplex having the 2-amino-Adap and dG combination did not show a clear melting behavior (Fig. 3A). Apparently, a stabilizing effect of 2-amino-Adap for dG is smaller than that of Adap in ODN**3** (Table 2, Entry 2 vs 6). It was also shown that 2-amino-Adap in ODN**4** exhibited a smaller stabilizing effect for both 8-oxo-dG and dG in telomere DNA**7** compared to Adap (Table 2, Entry 7 vs 11). Interestingly, when the T_m values were determined in a buffer containing 500 mM NaCl, ΔT_m obtained with 2-amino-Adap for 8-oxo-dG and dG became significantly larger than that obtained with Adap in a buffer containing 100 mM NaCl (Table 2, entry 3 vs 4; 19.2 vs 7.1 °C, entry 9 vs 10; 9.6 vs 7.1 °C). These results indicate that 2-amino-Adap in ODN**3** and **4** better discriminates 8-oxo-dG over dG in the telomere DNA.

Table 2
Thermal denaturing results for ODN**3** and **4** with the telomere DNA (**5**–**7**) containing 8-oxo-dG or dG[a]

Entry	**ODN**	Z	**DNA**	X	Y	T_m	ΔT_m
1	ODN**3**	2-Amino-Adap	DNA**5**	dG	8-Oxo-dG	43.4	>13.4
2			DNA**6**	dG	dG	<30	
3[b]		2-Amino-Adap	DNA**5**	dG	8-Oxo-dG	50.1	19.2
4[b]			DNA**6**	dG	dG	30.9	
5		Adap[c]	DNA**5**	dG	8-Oxo-dG	44.5	7.1
6			DNA**6**	dG	dG	37.4	
7	ODN**4**	2-Amino-Adap	DNA**7**	8-Oxo-dG	dG	37.7	>7.7
8			DNA**6**	dG	dG	<30	
9[b]		2-Amino-Adap	DNA**7**	8-Oxo-dG	dG	44.3	9.6
10[b]			DNA**6**	dG	dG	34.7	
11		Adap[c]	DNA**7**	8-Oxo-dG	dG	44.1	7.1
12			DNA**6**	dG	dG	37.0	

[a] UV-melting profiles measured using 1 μM ODN strand in a buffer containing 100 mM NaCl and 10 mM sodium phosphate at pH 7.0.
[b] The buffer here contains 500 mM NaCl and 10 mM sodium phosphate at pH 7.0.
[c] The T_m values of ODNs containing Adap are from Ref. 10b. $\Delta T_m = T_{m\ (8\text{-oxo-dG})} - T_{m\ (dG)}$. The sequences of DNA**5**–**7** are shown in the footnote to Figure 3.

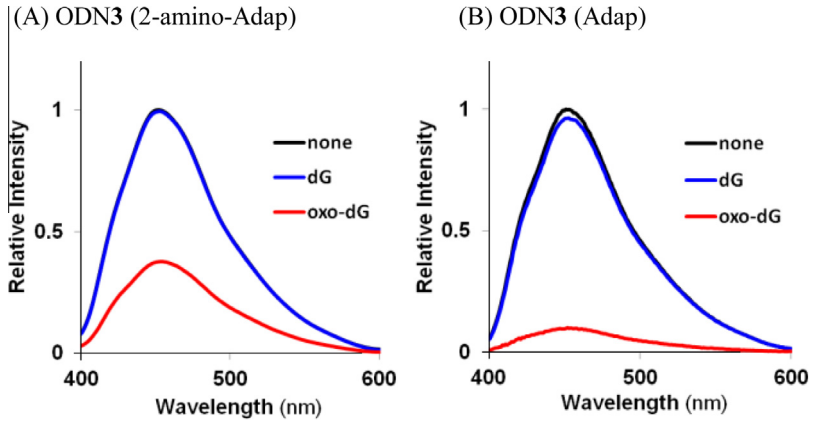

Figure 4. Fluorescence spectra of (A) 50 nM ODN**3** containing 2-amino-Adap and (B) 50 nM ODN**3** containing Adap in the same buffer conditions as in Figure 2. The black curves represent the spectra of single stranded ODN, the red curves show those after the addition of an 8-oxo-dG-containing sequence, and the blue curves show those after the addition of a dG-containing sequence.

2.5. Detection and quantification of 8-oxo-dG in the telomere DNA sequence

In our previous study, 8-oxo-dG in telomere DNA**5** was detected by the fluorescence quenching method, as shown in Figure 4B. Similarly, the fluorescence of 2-amino-Adap in ODN**3** (2-amino-Adap) was quenched by telomere DNA**5** containing 8-oxo-dG (Fig. 4A, red line) but was unresponsive to telomere DNA**6** containing dG (Fig. 4A, blue line). However, the quenching efficiency of 2-amino-Adap in ODN**3** was smaller than that of Adap in ODN**3** (Adap) (Fig. 4B, red line). Analogous to the discussion of the fluorescence intensity of ODN**1** and **2**, the fluorescence of 2-amino-Adap tends to be quenched in this ODN, most likely due to intrastrand stacking. Therefore, we focused on the large ΔT_m value between 8-oxo-dG and dG when complexed with 2-amino-Adap (Table 2, entries 1, 3 and 2, 4). Namely, a duplex is formed between ODN**3** (2-amino-Adap) and telomere DNA**5** (8-oxo-dG), whereas a duplex is only slightly formed between ODN**3** (2-amino-Adap) and telomere DNA**6** (dG) under the same conditions. SYBR Green in buffer emits strong fluorescence by binding with a duplex; thus, light-up detection of 8-oxo-dG in telomere DNA**5** is possible. Telomere DNA**5** containing 8-oxo-dG was added to a mixture of ODN**3** (2-amino-Adap) and SYBR Green in buffer at 30 °C, resulting in increased fluorescence intensity (Fig. 5A). In contrast, the fluorescence intensity of SYBR Green did not increase in a solution with the dG-containing telomere DNA**6** and ODN**3** (2-amino-Adap), indicating that no duplex had formed (Fig. 5B). Similar phenomena were observed with ODN**3** (Adap), except that fluorescence had slightly increased with telomere DNA**6** (dG) because ODN**3** (Adap) formed duplex DNA under the same conditions (Fig. 5C and D). The calibration curve was obtained using a constant ODN**3** (2-amino-Adap) concentration and a varied concentration of telomere

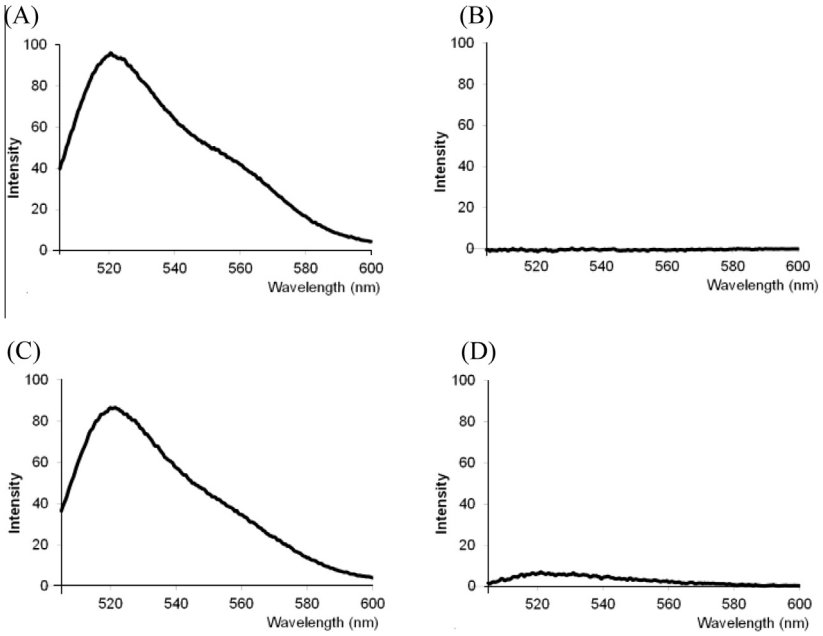

Figure 5. Light-up detection of 8-oxo-dG in telomere DNA**5** using SYBR Green. The combination of (A) 2-amino-Adap and 8-oxo-dG, (B) 2-aminoAdap and dG, (C) Adap and 8-oxo-dG and (D) Adap and dG. The fluorescence spectra were measured using 2 nM of each ODN with excitation at 494 nm in a buffer containing 100 mM NaCl and 10 mM sodium phosphate at pH 7.0 and 30 °C.

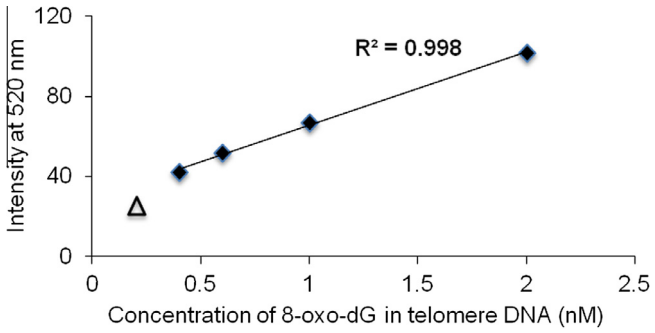

Figure 6. The calibration line of 8-oxo-dG in telomere DNA**5** using SYBR Green. The conditions are the same as in Figure 5 except that the concentrations of telomere DNA**5** are 0.2, 0.4, 0.6, 1.0 and 2.0 nM.

DNA**5** (8-oxo-dG), indicating a linear correlation in the range between 0.4 and 2.0 nM (Fig. 6, close diamond) with a detection limit of 0.2 nM (Fig. 6, open triangle).

3. Conclusion

In this study, we developed the 2-aminoadenosine derivative of 2-oxo-1,3-diazaphenoxazine (2-amino-Adap) for recognition of 8-oxo-dG in DNA in the anticipation of the formation of an additional hydrogen bond with the 8-oxo group of 8-oxo-dG. The recognition properties of ODNs containing 2-amino-Adap were investigated by measuring the T_m values and the fluorescence quenching. In contrast to the originally designed Adap, the base-pairing and fluorescence quenching properties of 2-amino-Adap were varied depending on the ODN sequence, and there was no clear indication that additional hydrogen bond formation with the 8-oxo group of 8-oxo-dG had occurred. Instead, the base-pairing of 2-amino-Adap with dG was significantly destabilized compared with the base-pairing of Adap with dG, resulting in a better selectivity for 8-oxo-dG in the human telomere DNA sequence. Thus, ODN**3** (2-amino-Adap) displayed selective, sensitive and quantitative detection of 8-oxo-dG in the human telomere DNA sequence, as indicated by the light-up detection system using SYBR Green.

4. Experimental Section

^{1}H NMR, ^{13}C NMR and ^{31}P NMR spectra were recorded on 400 MHz and 500 MHz NMR instruments using $CDCl_3$, CD_3OD or DMSO-d_6 as a solvent. High resolution mass (HRMS) was recorded on an EIS-TOF mass instrument in positive mode. MALDI-TOF data were collected in negative mode.

4.1. Synthesis of 2-amino-Adap phosphoramidite precursor

4.1.1. 3′,5′-Bis-*O*-*tert*-butyldimethylsilyl-2′-deoxy-O6-[(2,4,6-triisopropylphenyl)sulfonyl]-guanosine (2)

To a solution of 2′-deoxyguanosine (**1**) (5.0 g, 18.7 mmol) and imidazole (12.8 g, 187 mmol) in DMF (50 mL) was added *tert*-butyldimethylsilyl chloride (11.5 g, 74.8 mmol). After stirring for 24 h, the reaction mixture was diluted with EtOAc. The organic layer was washed with water and evaporated. The residue was purified by recrystallization from MeOH to provide **2** (6.8 g, 13.6 mmol, 73%) as a white solid. ^{1}H NMR (400 MHz, DMSO-d_6) δ (ppm) 7.85 (1H, s), 6.46 (1H, s), 6.09 (1H, t, J = 6.8 Hz), 4.48 (1H, br), 3.80 (1H, br), 3.61–3.91 (2H, m), 2.59–2.66 (1H, m), 2.20–2.25 (1H, m), 0.88 (9H, s), 0.86 (9H, s), 0.09 (6H, s), 0.03 (6H, s). This white solid **2** (5.0 g, 10.1 mmol) and triethylamine (2.2 mL, 30.3 mmol) were dissolved in CH_2Cl_2 (50 mL), and then 2,4,6-triisopropylphenylsulfonyl chloride (9.2 g, 30.3 mmol) and DMAP (154 mg, 1.3 mmol) were added to the reaction mixture at room temperature. After stirring for 48 h, the reaction mixture was diluted with EtOAc. The organic layer was washed with water, dried over Na_2SO_4, and evaporated under vacuum. The residue was purified by silica gel column chromatography (CH_2Cl_2/MeOH = 100/0–99/1) to give compound **2** (7.3 g, 9.6 mmol, 94%) as a white powder. ^{1}H NMR (400 MHz, CD_3OD) δ (ppm) 8.13 (1H, s), 7.29 (2H, s), 6.28 (1H, t, J = 6.2 Hz), 4.64 (1H, dt, J = 5.5, 3.7 Hz), 4.24 (2H, q, J = 6.7 Hz), 3.96–3.93 (1H, m), 3.82 (1H, dd, J = 11.0, 3.7 Hz), 3.76 (1H, dd, J = 11.0, 3.7 Hz), 2.95 (1H, q, J = 6.7 Hz), 2.73 (1H, ddd, J = 13.3, 6.7, 6.2 Hz), 2.39 (1H, ddd, J = 13.3, 6.2, 4.0 Hz), 1.26 (6H, d, J = 6.7 Hz), 1.24 (12H, d, J = 6.7 Hz), 0.92 (9H, s), 0.87 (9H, s), 0.13 (6H, s), 0.05 (3H, s), 0.03 (3H, s). ^{13}C NMR (125 MHz, DMSO-d_6) δ (ppm) 159.1, 156.3, 155.6, 144.5, 141.0, 140.7, 133.2, 132.3, 117.3, 88.5, 84.5, 72.6, 63.5, 41.5, 26.6, 26.4, 23.4, 21.8, 19.1, 18.7, −4.0, −4.1, −4.7, −4.8. HRMS (m/z) calcd for $C_{37}H_{64}N_5O_6SSi_2$ $(M+H)^+$ 762.4110, found 762.4150.

4.1.2. 3′,5′-Bis-*O*-*tert*-butyldimethylsilyl-2′-deoxy-6-*N*-{2-[(1,3-diaza-3-methyl-2-oxo-phenoxazine-9-yl)oxy]-ethyl}-2-amino-adenosine (4)

A reaction mixture of **2** (870 mg, 1.14 mmol), phenoxazine unit **3** (209 mg, 0.76 mmol) and DIPEA (0.20 mL, 1.14 mmol) in 1-propanol (3.5 mL) was refluxed at 100 °C for 12 h. The reaction was quenched by saturated aqueous $NaHCO_3$. The 1-propanol was removed under reduced pressure. The aqueous layer was extracted with EtOAc. The organic layer was repeatedly washed with water and brine, dried over Na_2SO_4, and evaporated under vacuum. The residue was purified by silica gel column chromatography (Hexane/EtOAc = 10/1 to 1/1) to give compound **4** (503 mg, 0.67 mmol, 88%) as a yellow powder. ^{1}H NMR (400 MHz, CD_3OD) δ (ppm): 7.92 (1H, s), 7.06 (1H, br s), 6.78 (1H, t, J = 8.0 Hz), 6.59 (1H, d, J = 8.0 Hz), 6.37 (1H, d, J = 8.0 Hz), 6.28 (1H, t, J = 6.4 Hz), 4.62–4.59 (1H, m), 4.30–4.20 (2H, m), 3.96 (1H, dd, J = 7.6, 3.6 Hz), 3.87–3.77 (4H, m), 3.22 (3H, s), 2.59–2.55 (1H, m), 2.41–2.36 (1H, m), 0.94 (9H, s), 0.87 (9H, s), 0.10 (6H, s), 0.06 (6H, d, J = 8.4 Hz). ^{13}C NMR (125 MHz, CD_3OD) δ (ppm) 161.8, 156.3, 137.0, 129.9, 129.4, 124.5, 114.9, 109.6, 103.9, 89.2, 84.9, 73.6, 64.2, 42.1, 30.8, 27.5, 26.5, 26.3, 25.4, 19.2, 18.9, 1.50, −4.02, −4.43, −4.56, −5.27, −5.32. HRMS (m/z) calcd for $C_{35}H_{54}N_9O_6Si_2$ $(M+H)^+$ 752.3730, found 752.3745.

4.1.3. 2′-Deoxy-6-*N*-{2-[(1,3-diaza-3-methyl-2-oxo-phenoxazine-9-yl)oxy]-ethyl}-2-phenoxyacetylamino-adenosine (5)

Phenoxyacetyl chloride (0.17 mL, 0.50 mmol) was added to a solution of **4** (376 mg, 0.50 mmol) in pyridine (5.0 mL) at 0 °C. After stirring for 24 h at room temperature, the reaction was quenched by saturated aqueous $NaHCO_3$ and extracted with CH_2Cl_2. The organic layer was washed with brine, dried over Na_2SO_4, and evaporated under vacuum. The residue was then washed with Et_2O to give a yellow powder (324 mg, 0.44 mmol, 88%). This yellow powder (300 mg, 0.41 mmol) was treated with triethylamine-trihydrofluoride (0.11 mL, 0.70 mmol) in THF (3.5 mL). After stirring for 2 h, the organic layer was evaporated under vacuum. The residue was purified by silica gel column chromatography ($CHCl_3$/MeOH = 100/1 to 10/1) to give compound **5** (243 mg, 0.33 mmol, 90%) as a yellow powder. ^{1}H NMR (400 MHz, DMSO-d_6) δ (ppm) 10.12 (1H, s), 9.92 (1H, br s), 8.49 (1H, br s), 8.28 (1H, s), 7.47 (1H, br s), 7.29 (2H, t, J = 8.0 Hz), 6.93 (3H, m), 6.74 (1H, t, J = 8.2 Hz), 6.56 (1H, d, J = 8.2 Hz), 6.40 (1H, d, J = 8.2 Hz), 6.28 (1H, t), 5.27 (1H, d), 5.04 (2H, br s), 4.91–4.87 (1H, m), 4.40–4.36 (1H, m), 4.08–4.05 (2H, m), 3.88 (1H, br s), 3.84–3.80 (1H, m), 3.60–3.47 (2H, m), 3.18 (3H, s), 2.65–2.63 (1H, m), 2.49–2.47 (1H, m). ^{13}C NMR (125 MHz, DMSO-d_6) δ (ppm) 167.6, 157.9,

154.3, 152.4, 149.4, 149.4, 142.3, 138.4, 129.4, 125.8, 122.8, 120.8, 115.0, 114.5, 107.7, 106.7, 87.7, 83.0, 70.7, 67.4, 61.7, 59.9, 36.5, 14.0. HRMS (*m*/*z*) calcd for $C_{31}H_{32}N_9O_8$ $(M+H)^+$ 658.2368, found 658.2334.

4.1.4. 2′-Deoxy-5'-*O*-dimethoxytrityl-6-*N*-{2-[(1,3-diaza-3-methyl-2-oxo-phenoxazine-9-yl)oxy]-ethyl}-2-phenoxyacetylamino-adenosine-3′-(2-cyanoethyl-N,N-diisopropylphosphoramidite) (6)

To a solution of the corresponding diol **5** (190 mg, 0.29 mmol) in pyridine (3 mL) was added DMTrCl (118.6 mg, 0.35 mmol). After stirring for 1 h, the reaction mixture was diluted with EtOAc. The organic layer was repeatedly washed with water and a satd NaCl solution, dried over Na_2SO_4, and then evaporated under reduced pressure. The residue was purified by flash column chromatography ($CHCl_3$/MeOH = 100/0 to 20/1) to give the DMTr-protected compound as a yellow foam (178.4 mg, 0.19 mmol, 64%). The DMTr-protected compound was dissolved in CH_2Cl_2 (3.5 mL) and diisopropylethylamine (0.19 mL, 1.10 mmol) at 0 °C. After stirring for 15 min at the same temperature, *N*,*N*-diisopropylchlorophosphoramidite (0.12 mL, 0.55 mmol) was added to the reaction mixture, which was stirred for 1 h at room temperature. The reaction mixture was diluted with EtOAc, and the organic layer was washed with a sat. $NaHCO_3$ solution, dried over Na_2SO_4, and then evaporated under reduced pressure. The residue was purified by flash column chromatography ($CHCl_3$/MeOH = 100/0 to 20/1) to give a pale yellow foam. This foam was dissolved in CH_2Cl_2 and poured into hexane at −78 °C. The resulting white powder was collected and dried under vacuum to give the corresponding amidite precursor **6** (190.4 mg, 0.16 mmol, 88%). ^{1}H NMR (400 MHz, $CDCl_3$) δ (ppm) 8.36 (1H, br), 8.18 (1H, br), 7.37–7.35 (2H, m), 7.32–7.25 (4H, m), 7.24–7.10 (4H, m), 7.01–6.97 (3H, m), 6.78–6.71 (6H, m), 6.43 (1H, d, *J* = 7.6 Hz), 6.34–6.31 (2H, m), 4.89 (1H, br), 4.65 (1H, br), 4.23–4.07 (5H, m), 3.82 (2H, s), 3.71 (6H, t, *J* = 2.0 Hz), 3.60–3.44 (4H, m), 3.37–3.27 (2H, m), 3.15 (3H, s), 2.79–2.72 (3H, m), 2.67–2.52 (2H, m), 2.41 (1H, t, *J* = 6.4 Hz), 1.56 (12H, s). ^{31}P NMR (162 MHz, $CDCl_3$) δ (ppm) 148.7. HRMS (*m*/*z*) calcd for $C_{61}H_{67}N_{11}O_{11}P$ $(M+H)^+$ 1160.4754, found 1160.4718.

4.2. Synthesis of ODNs containing 2-amino-Adap

ODNs were synthesized by standard DNA synthesis procedures. After synthesis of ODN, the resin was treated with 28% ammonium solution at 55 °C for 6 h. The crude product was purified by HPLC to obtain pure DMTr-ODN. The DMTr-group was then cleaved in 5% acetic acid at room temperature, and the resulting DMTr-OH was removed by washing with ether. The purities and structures of each synthesized ODN were identified by MALDI-TOF analysis. ODN**1** (2-amino-Adap): calcd 4095.67, found 4095.49, ODN**2** (2-amino-Adap): calcd 4358.86, found 4358.58, ODN**3** (2-amino-Adap): calcd 4733.85, found 4733.74, ODN**4** (2-amino-Adap): calcd 4733.85, found 4733.64. Other ODNs and target DNAs were purchased from Japan Bio Services Co., LTD.

4.3. T_m measurements

Duplex DNA was heated to 90 °C for 5 min and annealed by slow cooling in 10 mM sodium phosphate buffer containing 100 mM NaCl or 500 mM NaCl at pH 7.0 prior to the T_m measurement. The temperature was raised from 10 °C to 80 °C at a rate of 1.0 °C/min and the UV absorbance was monitored at 260 nm. The T_m values were obtained by the analysis of the melting curve with MeltWin(v3.5). Thermodynamic parameters summarized in Table 1 were calculated from the T_m values obtained using the different concentration of duplex DNA at 1, 2, 3, 5 and 8 μM. The T_m values summarized in Table 2 were obtained using 1 μM of duplex DNA.

4.4. Fluorescence measurements

The fluorescence spectra displayed in Figures 2 and 4 were measured using 50 nM of each ODN in the buffer containing 100 mM NaCl with 10 mM sodium phosphate at pH 7.0 and 30 °C with excitation wavelength at 365 nm.

4.5. CD measurements

CD spectra were measured using 5.0 μM of each ODN in the buffer containing 100 mM NaCl and 10 mM sodium phosphate at pH 7.0 and 25 °C. The black line shows the single stranded target DNA**5** and **6** containing 8-oxo-dG and dG, respectively. The red line shows the mixture of corresponding target DNA and ODN**3** containing 2-amino-Adap.

4.6. Detection and quantification of duplex formation by fluorescence measurements using SYBR Green I

A mixture of ODN**3** (2-amino-Adap or Adap) (2 nM) and SYBR Green was stirred for 10 min in buffer containing 100 mM NaCl and 10 mM sodium phosphate at pH 7.0 and 30 °C. After addition of telomere DNA containing 8-oxo-dG or dG (2 nM) and stirring for 10 min at 30 °C, the fluorescence spectrum was recorded with excitation at 494 nm. The construction of a calibration curve was plotted for fluorescence intensity values at 520 nm using different concentrations of the telomere DNA**5** from 0.2 to 2.0 nM. The straight line and the R^2 values were calculated using linear regression for the data between 0.4 and 2.0 nM, and are shown in Figure 6.

Acknowledgments

This study was supported by a Grant-in-Aid for Scientific Research (S) (Grant Number 21229002 for S.S.) and Challenging Exploratory Research (Grant Number 24659047 for Y.T.) from the Japan Society for the Promotion of Science (JSPS). Y.T. acknowledges support from a Kyushu University Interdisciplinary Program in Education and Projects in Research Development (P&P).

Supplementary data

Supplementary data (^{1}H NMR spectrum of new compound **2**, **4**, **5** and **6**) associated with this article can be found, in the online version, at http://dx.doi.org/10.1016/j.bmc.2014.01.024.

References and notes

1. (a) Lindahl, T. *Nature* **1993**, *362*, 709; (b) Cooke, M. S.; Evans, M. D.; Dizdaroglu, M.; Lunec, J. *FASEB J.* **2003**, *17*, 1195.
2. Neeley, W. L.; Essigmann, J. M. *Chem. Res. Toxicol.* **2006**, *19*, 491.
3. Lu, A.-L.; Li, X.; Gu, Y.; Wright, P. M.; Chang, D.-Y. *Cell Biochem. Biophys.* **2001**, *35*, 141.
4. Hofer, T.; Seo, A. Y.; Prudencio, M.; Leeuwenburgh, C. *Biol. Chem.* **2006**, *387*, 103.
5. Simoeki, A.; Rytarowska, A.; Poplawska, A. S.; Gackowski, D.; Rozalski, R.; Dziaman, T.; Szaflarska, M. C.; Olinski, R. *Carcinogenesis* **2006**, *27*, 405.
6. Malayappa, B.; Garrett, T. J.; Segal, M.; Leeuwenburgh, C. *J. Chromatogr. A* **2007**, *1167*, 54.
7. (a) Yoshida, R.; Ogawa, Y.; Kasai, H. *Cancer Epidemiol. Biomarkers Prev.* **2002**, *11*, 1072; (b) Shimoi, K.; Kasai, H.; Yokota, N.; Toyokuni, S.; Kinae, N. *Cancer Epidemiol. Biomarkers Prev.* **2002**, *11*, 767.
8. (a) Poulsen, H. E.; Nadal, L. L.; Broedbaek, K.; Nielsen, P. E.; Weimann, A. *Biochim. Biophys. Acta* **2014**, *1840*, 801; (b) Michel, C.; Vincent-Hubert, F. *Mutat. Res.* **2012**, *741*, 1; (c) Hah, S. S.; Mundt, J. M.; Kim, H. M.; Sumbad, R. A.; Turteltaub, K. W.; Henderson, P. T. *Proc. Natl. Acad. Sci. U.S.A.* **2007**, *104*, 11203.
9. (a) Nakagawa, O.; Ono, S.; Li, Z.; Tsujimoto, A.; Sasaki, S. *Angew. Chem., Int. Ed.* **2007**, *46*, 4500; (b) Li, Z.; Nakagawa, O.; Koga, Y.; Taniguchi, Y.; Sasaki, S. *Bioorg. Med. Chem.* **2010**, *18*, 3992; (c) Nasr, T.; Li, Z.; Nakagawa, O.; Taniguchi, Y.; Ono, S.; Sasaki, S. *Bioorg. Med. Chem. Lett.* **2009**, *19*, 727.
10. (a) Taniguchi, Y.; Kawaguchi, R.; Sasaki, S. *J. Am. Chem. Soc.* **2011**, *133*, 7272; (b) Erratum *J. Am. Chem. Soc.* **2011**, *133*, 10322.

11. Taniguchi, Y.; Koga, Y.; Fukabori, K.; Sasaki, S. *Bioorg. Med. Chem. Lett.* **2012**, *22*, 543.
12. Cheong, C.; Tinoco, I., Jr.; Chollet, A. *Nucleic Acids Res.* **1988**, *16*, 5115.
13. (a) Oikawa, S.; Tada-Oikawa, S.; Kawanishi, S. *Biochemistry* **2001**, *40*, 4763; (b) Oikawa, S.; Kawanishi, S. *FEBS Lett.* **1999**, *453*, 365.
14. Vorlickova, M.; Tomasko, M.; Sagi, A. J.; Bednarova, K.; Sagi, J. *FEBS J.* **2012**, *279*, 29.